Effect of standing-wave field distribution on femosecond laser-induced damage of HfO_2/SiO_2 mirror coating

Shunli Chen (陈顺利)[1,2], Yuan'an Zhao (赵元安)[1*], Hongbo He (贺洪波)[1], and Jianda Shao (邵建达)[1]

[1] *Key Laboratory of Materials for High Power Laser, Shanghai Institute of Optics and Fine Mechanics, Chinese Academy of Sciences, Shanghai 201800, China*

[2] *Graduate University of Chinese Academy of Sciences, Beijing 100049, China*

[*] *Corresponding author: yazhao@siom.ac.cn*

Received December 31, 2010; accepted March 15, 2011; posted online May 31, 2011

Single-pulse and multi-pulse damage behaviors of "standard" (with $\lambda/4$ stack structure) and "modified" (with reduced standing-wave field) HfO_2/SiO_2 mirror coatings are investigated using a commercial 50-fs, 800-nm Ti:sapphire laser system. Precise morphologies of damaged sites display strikingly different features when the samples are subjected to various number of incident pulses, which are explained reasonably by the standing-wave field distribution within the coatings. Meanwhile, the single-pulse laser-induced damage threshold of the "standard" mirror is improved by about 14% while suppressing the normalized electric field intensity at the outmost interface of the HfO_2 and SiO_2 layers by 37%. To discuss the damage mechanism, a theoretical model based on photoionization, avalanche ionization, and decays of electrons is adopted to simulate the evolution curves of the conduction-band electron density during pulse duration.

OCIS codes: 310.1620, 320.7090, 140.3330, 260.3230.

doi: 10.3788/COL201109.083101.

In the chirped pulse amplification (CPA) and optical parametric CPA (OPCPA) laser systems, multilayer dielectric mirror coatings serve as the fundamental part of multilayer dielectric pulse compressor gratings and ultra-broadband mirrors[1]. Laser-induced damage of dielectric coatings has always been a limiting factor for the constant and stable operation of high-power laser system[2−6]. Consequently, enhancing the laser resistance of coatings becomes distinctly important. However, there are only a few studies dedicated to improving the laser-induced damage threshold (LIDT) of mirror coatings in the femosecond (fs) regime. Laser conditioning was verified to be invalid for mirror coatings because neither long-pulse nor short-pulse conditioning resulted in higher LIDT[7]. Moreover, low refractive index protective layer, such as half-wave SiO_2 single layer, was tried by Yuan *et al.*[8]. Unfortunately, it was found that the SiO_2 protective layer had no positive effect on improving the LIDT of mirrors.

From the 70s of the last century, a method for improving the LIDT of multilayer coatings was adopted by suppressing the peak electric field intensity within the critical layers[9,10]. In recent years, some investigations have been conducted focusing on the relation between the fs laser-induced damage and the standing-wave electric field distribution within dielectric coatings[11,12]. It was also demonstrated to be effective by reducing the electric field intensity at the interfaces of high-index and low-index materials to increase the LIDT for both Ta_2O_5/SiO_2 and HfO_2/SiO_2 multilayer dielectric high-reflective mirrors[12]. However, only the multi-pulse damage behavior of samples was discussed extensively and correlative research on the single-pulse damage of high-reflective coatings was incomplete. Therefore, more comprehensive studies on the damage of coatings, including single-pulse damage test, are necessary. Some interesting physics was observed from the single-pulse damage experiment in this letter.

In this letter, HfO_2 was used as a high-index material to realize high-reflective mirrors due to its relatively high LIDT, and good thermal and mechanical stability[13]. Two kinds of HfO_2/SiO_2 mirrors, one with "standard" (with $\lambda/4$ stack structure) design and the other with "modified" (with reduced standing-wave field) design, were prepared by electron beam evaporation (EBE) technology. A 50-fs, 10-Hz, 800-nm Ti:sapphire laser system was used to study the single-pulse and multi-pulse damage behaviors of these coatings. Optical microscope, scanning electron microscopy (SEM), and surface profiler were employed to confirm the damage features of the samples. In addition, a theoretical model was adopted to illustrate the fs laser-induced damage mechanism.

All the samples were prepared from HfO_2 and SiO_2 materials with refractive indices of 1.98 and 1.44 at the wavelength of 800 nm, and optical band gaps of 5.4 and 8.3 eV, respectively. All the samples were obtained at the same deposition conditions by EBE. The beam currents were 120 mA for HfO_2 and 60 mA for SiO_2. Moreover, the substrate temperature was kept at 200 °C during deposition, while the deposition rates of HfO_2 and SiO_2 target materials were 0.3 and 0.6 nm/s, respectively. The deposition pressure of background gas O_2 in the coating chamber was 2×10^{-2} Pa. The structure of the "standard" mirror was given by $G||(HL)^{12}H||Air$, where G denoted BK7 glass substrate (30×3 (mm)), and H and L standed for the high-refractive index material (HfO_2) and the low-refractive index oxide (SiO_2), respectively, with quarter wavelength optical thickness (QWOT).

In order to lower the electric field intensity at outer interfaces within the "modified" mirror, we modified the relative thicknesses of the H and L layers for the outer six layers to shift the electric field peaks to more resistant low-refractive index SiO_2 material. The coatings were designed by commercially available thin film software

"TFCalc". The initial desired destination was to reduce the normalized electric field intensity (NEFI) by 50% at the outmost layer interface while keeping the magnitude of the NEFI at the inner interfaces moderate. Perkin Elmer Lambda 900 UV/VIS/NIR spectrometer was employed to test the optical properties of the samples for damage experiments. The spectra data of the two kinds of coatings and the corresponding electric field distribution are shown in Figs. 1 and 2, respectively.

Notice that the measured reflective spectrum agreed very well with the designed curve for the "standard" mirror. However, for the "modified" mirror, compared with the designed spectrum, the obtained curve revealed a little shift toward shorter wavelength due to the total deposition thickness error of ±0.6%. Such experimental error led to the measured total thickness of the "modified" coating to be 20 nm less than the designed value, which resulted in the obtained NEFI of the "modified" mirror being suppressed merely by 37% at the outmost layer interface.

A 50-fs, 10-Hz, 800-nm CPA Ti:sapphire laser system was applied to generate fundamental laser radiation with near-Gaussian spatial profile (Fig. 3)[8]. A half-wave plate and a polarizing beam splitter combination worked as a variable attenuator for varying the laser energy. An isolated mechanical shutter needed a number of pulses from the output 10-Hz pulse train. The pulse energy was measured by an energy meter from a split-off portion of the beam. The specimen for damage measurement was

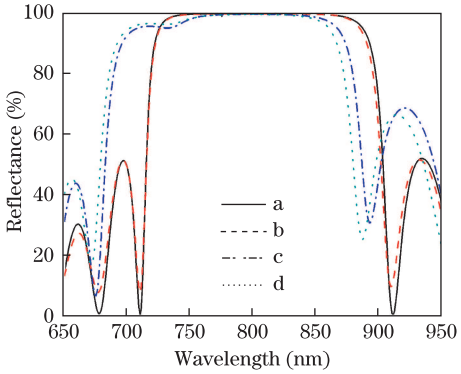

Fig. 1. Measured and designed spectra of experimental HfO_2/SiO_2 mirrors. Curves "a" and "b" stand for the designed and measured spectra of "standard" mirror; curves "c" and "d" stand for the designed and measured spectra of "modified" mirror.

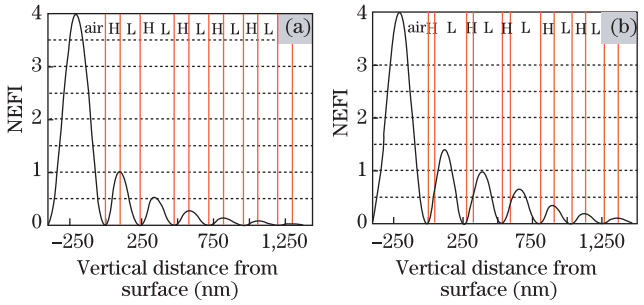

Fig. 2. Obtained distribution of NEFI in the six pairs of outer layers of HfO_2/SiO_2 mirrors. The incident light wavelength is 800 nm with 0° incident angle. (a) "Standard" and (b) "modified" designs.

mounted on a motorized $x-y$ translation stage. The surface of the specimen was positioned perpendicular to the direction of the incident laser beam in the focal plane of a lens with focal length of 4 m and was monitored *in situ* with a charge-coupled device (CCD) and a cold light source in order to avoid heating the sample. The Gaussian spatial beam profile with a radius ($1/e^2$) of ~1 mm was achieved. The occurrence of damage onset was ascertained by Leica optical microscope, and specific damage images were observed by the SEM (JSM-6360LA) and WYKO surface profiler.

Single-pulse damage experiment was implemented by irradiating only one pulse onto one sample spot; meanwhile, for multi-pulse test, 40 pulses with fixed energy fluence were irradiated onto the same sample spot. The LIDT of the experimental specimen was determined similar to the ablation threshold fluence by the relation of the damage spot area and the laser fluence, namely, measuring the diameter of the damage crater versus the pulse fluence and then extrapolating to zero. The relative error of the LIDT determination amounts to ±9%, mainly due to the uncertainty of the damage crater size measurement. The damage morphologies of two kinds of mirrors for both single-pulse and multi-pulse experiments were explained in details. Only the LIDT of the single-pulse experiment was calculated because our theoretical model to simulate the evolution curves of the conduction-band electron density during pulse duration was merely appropriate for the single-pulse damage of materials.

For the single-pulse damage experiment, near the LIDT, contour graphs information of damaged sites indicated that the damage depth was approximately equivalent to the thickness of the outmost HfO_2 material for the "standard" mirror with flat-bottomed crater. For the "modified" reflector, the crater depth almost approached to the peak location of the NEFI in the outmost SiO_2 layer with cone-shape damage pit. Clearly, their typical morphologies show significant distinction (Fig. 4). The damage crater of the "standard" mirror presents the outmost HfO_2 layer exfoliated entirely at the center of the Gaussian pulse profile (Fig. 4(a1)), while the fringe boundary of the damage spot is clear cut and legible (Fig. 4(a2)). Contrast is clear that the typical damage pit of the "modified" mirror appears to be a scattered spalling feature from the center to the fringe region of the incident pulse (Fig. 4(b1)). Simultaneously, its edge area displays ambiguous and illegible characteristics (Fig. 4(b2)).

The clearly distinctive features of the two kinds of coatings could be explained reasonably by standing-wave field distribution near the outmost interface between the HfO_2 and SiO_2 layers. For the "standard" mirror, the peaks of the NEFI are located exactly at the interface areas (Fig. 2(a)). The outmost interface with the maximum

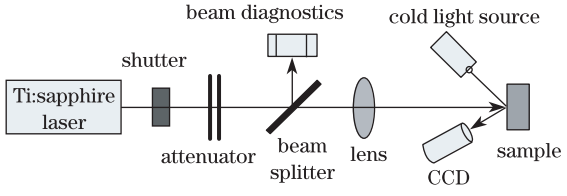

Fig. 3. Schematic diagram of fs-laser damage tests facility.

peak is most likely to be damaged. Hence, near the LIDT, laser pulse with fluence of 0.47 J/cm^2 only led to the damage of the outmost HfO_2 layer, which was entirely exfoliated from the inner layers at the center of the Gaussian pulse. On the other hand, for the "modified" coating, the peaks of the NEFI were shifted to the low-refractive index SiO_2 layer. As a result, the outer interfaces between the HfO_2 and SiO_2 layers presented moderate NEFI (Fig. 2(b)) compared with that of the adjacent SiO_2 layer. Consequently, the laser resistance of the outer interfaces was enhanced, and the tendency of the outmost HfO_2 layer exfoliated directly from the inner layers was weakened. Furthermore, the irregularities at the boundary region of the ablation crater may be the result of the damage competition between the HfO_2 material at the outmost interface and the SiO_2 material with the maximum peak NEFI in the adjacent layer. This means that the interfacial HfO_2 material (band gap 5.4 eV) performs feeble laser resistance but only needs to undergo low NEFI, whereas the adjacent SiO_2 material (band gap 8.3 eV) appeares to have relatively stronger intrinsic laser resistance but has to experience much higher NEFI—nearly two times that of the interface location. Hence, incident laser pulse with fluence of 0.47 J/cm^2 seemed to trigger the nearly waxing and waning exfoliation of the interfacial HfO_2 and the adjacent SiO_2 materials, while the damage competition manifested a clear scattered spalling feature at the boundary region by the relatively lower near-threshold energy fluence. Additionally, most of the layer materials at the center area of the Gaussian-shape pulse were peeled off due to relative higher energy fluence.

For multi-pulse damage test, different damage characteristics can also be identified easily between the "standard" mirror (Figs. 5(a1) and (a2)) and the "modified" coating (Figs. 5(b1) and (b2)). The representative cone-shape damage crater of the "standard" mirror appeared with layered flake-off from the center to the fringe region of the incident pulse, which was believed to be associated with the step-decrease feature of the NEFI from the outer to the inner interfaces (Fig. 2(a)). Thus, the critical electron density at the interfaces of the outer layers due to higher NEFI could be reached by the lower energy fluence present at the peripheral area of the pulse with the Gaussian-shape spatial profile, whereas the inner layers require higher fluence present at the very center of the pulse[12]. In sharp contrast with the "standard" mirror, typical cylinder-like damage pits of the "modified" coating displayed several layers being damaged simultaneously, which was considered to be determined by the gradual decrease in the NEFI from the outer to the inner interfaces, especially by the approximately equal NEFI at the outer four interfaces between the HfO_2 and SiO_2 layers (Fig. 2(b)). This means that the critical conditions are reached at the same time at several outer layer interfaces.

The calculated single-pulse LIDT of the "standard" mirror was nearly 14% higher than that of the "modified" coating while suppressing the NEFI at the outmost interface of the HfO_2 and SiO_2 layers by 37%. A similar result from the multi-pulse experiment was described for the HfO_2/SiO_2 mirror with the overcoat of half-wavelength SiO_2 layer, while the LIDT of the "standard" mirror was improved by 12% after suppressing the electric field two times[12]. In the fs-pulse regime, the highly deterministic damage performance is considered to be closely related to the nonlinear ionization processes, such as photoionization (PI), avalanche ionization (AI), and decays of electrons associated with the diffusion and recombination of electrons[14,15]. This can be explained by the nonlinear excitation of electrons to the conduction band via these nonlinear ionization procedures. When the electron density of the conduction band reaches a critical plasma density n_{cr}, the respective plasma waves are resonant with the incident laser wavelength. Hence, the material absorbs laser radiation strongly through the process of inverse bremsstrahlung, resulting in permanent structural changes and material damage. Because the damage of all the samples is primarily due to the intrinsic properties of their coatings, the combination of these different ionization mechanisms contributes to the final damage of materials. In addition, the damage behavior of the two kinds of mirrors confirmed that the damage process is largely linked to the distribution of the standing-wave field within these coatings. Consequently, the correction factor that considers interference effects within the coatings should be included. For the "standard" and "modified" mirrors, the correction factors of the standing-wave electric field were extracted from the outmost interfaces of the H and L layers, which were identified to be the weakest position producing

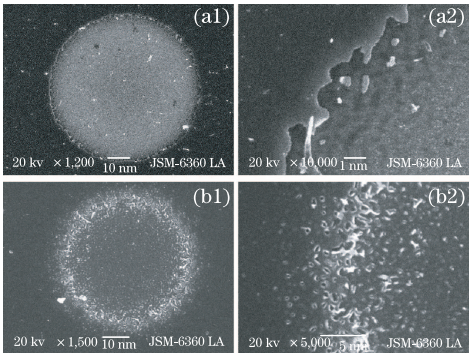

Fig. 4. Typical damage morphologies of HfO_2/SiO_2 mirrors for single-pulse test. The incident pulse fluence is 0.47 J/cm^2. (a1) "Standard" mirror; (a2) fringe information in (a1); (b1) "modified" mirror; (b2) fringe information in (b1).

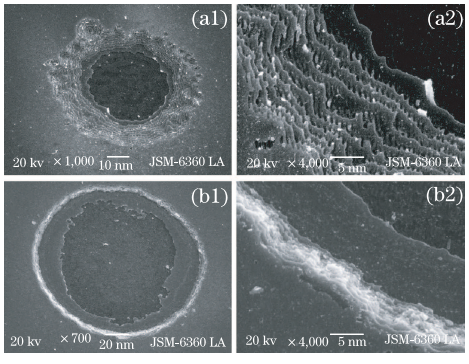

Fig. 5. Typical damage morphologies of HfO_2/SiO_2 mirrors for 40-pulse test. The incident pulse fluence is 0.39 J/cm^2. (a1) "Standard" mirror; (a2) fringe information in (a1); (b1) "modified" mirror; (b2) fringe information in (b1).

initial damage. As a result, in order to discuss the damage mechanism, a theoretical model based on PI, AI, and decays of electrons was adopted to simulate the evolution curves of the conduction-band electron density in material during pulse duration. The critical plasma density is represented by[15]:

$$n_{\rm cr} = (\varepsilon_0 m_{\rm e}^* \omega^2)/e^2, \quad (1)$$

where ε_0 is the permittivity of free space, $m_{\rm e}^*$ denotes the effective electron mass, and ω and e stand for the incident laser frequency and the electron charge, respectively.

The rate equation of electron excitation to the conduction band in multilayer coatings exposed to fs laser pulses is written as

$$\frac{\partial n_{\rm e}}{\partial t} = W_{\rm PI\_Keldysh} + W_{\rm AI\_Drude} \cdot n_{\rm e}(t) - \frac{n_{\rm e}(t)}{\tau_r}, \quad (2)$$

where $n_{\rm e}(t)$ denotes the electron density, $W_{\rm PI\_Keldysh}$ stands for the PI rate described by the Keldysh theory[16], and $W_{\rm AI\_Drude}$ is the AI rate calculated according to Drude's ionization model[17]. The last term, $[n_e(t)/\ \tau_r]$, indicates the plasma decays with the relaxation time τ_r =100 fs[14]. In addition, for the "standard" and "modified" mirrors, the correction factors of the electric field extracted from the outmost interface of the H and L layers were 1.02 and 0.64, respectively (Figs. 2(a) and (b)), which, as factors of the electric field amplitude, were taken into detailed rate equations when simulating.

In the theoretical calculation, the reduced effective mass $m_{\rm e}^*$ of the conduction electron and valence hole for both HfO_2 and SiO_2 materials is $0.5m_0$, where m_0 is the free-electron mass[8]. Figuer 6 displays the total evolution of electron density for the time period of the laser pulse in the two kinds of mirrors, which is produced by an 800-nm, 50-fs laser pulse with the peak intensity I_0= 6.57 TW/cm^2. For the identical laser parameters, when the electron density of the "standard" mirror achieves a level of critical electron density, leading to the occurrence of dielectric damage, the electron density in the "modified" coating is almost three orders of magnitude smaller than that of the "standard" mirror. It is clear that the ionization rate of the "standard" mirror is larger than that of the "modified" coating irradiated by the same laser pulse, which confirms that the LIDT of the "modified" coating appears distinctly higher than that of the "standard" mirror.

In conclusion, for the single-pulse test, the damage crater of the "standard" mirror shows the entire exfoliation of the outmost HfO_2 layer from the center to the fringe region of the Gaussian pulse, whereas that of the "modified" coating appeares to be a scattered spalling feature. Meanwhile, for the multi-pulse test, the "standard" and "modified" mirrors show typical cone-shape crater and cylinder-like pit, respectively. These results are illustrated reasonably by different standing-wave field distribution within these coatings. Moreover, the LIDT of the HfO_2/SiO_2 mirror for single-pulse damage is improved by about 14% while suppressing the peak of NEFI at the outmost interface of HfO_2 and SiO_2 materials by 37%. To explain the damage mechanism

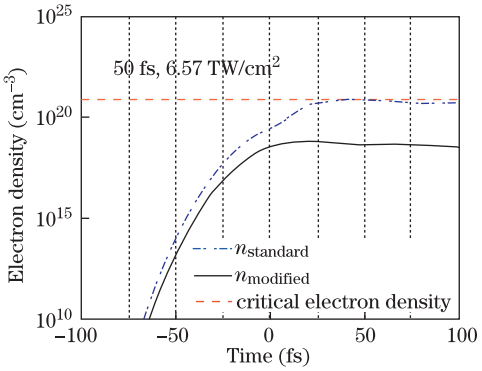

Fig. 6. Evolution of electron density in HfO_2/SiO_2 mirrors for "standard" design (dot-dashed line) and "modified" design (dashed line) coatings during a 50-fs, 800-nm laser pulse; the calculated critical electron density (solid line) from Eq. (1) ($\sim 10^{21}$ cm^{-3}) is shown as the damage criterion.

qualitatively, a theoretical model based on photoionization, avalanche ionization, and decays of electrons is adopted to simulate the evolution curves of the conduction-band electron density during pulse duration.

References

1. H. Zeng, J. Wu, H. Xu, K. Wu, and E. Wu, Appl. Phys. B **79,** 837 (2004).
2. T. W. Walker, A. H. Guenther, and P. E. Nielsen, IEEE J. Quantum Electron. **17,** 2041 (1981).
3. J. Jasapara, A. V. V. Nampoothiri, and W. Rudolph, Phys. Rev. B **63,** 045117 (2001).
4. C. Huang, Y. Xue, Z. Xia, Y. Zhao, F. Yang, and P. Guo, Chin. Opt. Lett. **7,** 49 (2009).
5. G. Dai, Y. Chen, J. Lu, Z. Shen, and X. Ni, Chin. Opt. Lett. **7,** 601 (2009).
6. X. Liu, D. Li, Y. Zhao, X. Li, X. Ling, and J. Shao, Chin. Opt. Lett. **8,** 41 (2010).
7. B. C. Stuart, M. D. Feit, S. Herman, A. M. Rubenchik, B. W. Shore, and M. D. Perry, J. Opt. Soc. Am. B **13,** 459 (1996).
8. L. Yuan, Y. Zhao, C. Wang, H. He, Z. Fan, and J. Shao, Appl. Surf. Sci. **253,** 3450 (2007).
9. J. H. Apfel, Appl. Opt. **16,** 1880 (1977).
10. F. Demichelis, E. Mezzetti-Minetti, L. Tallone, and E. Tresso, Appl. Opt. **23,** 165 (1984).
11. K. Starke, T. Gross, and D. Ristau, Proc. SPIE **4347,** 528 (2001).
12. G. Abromavicius, R. Buzelis, R. Drazdys, A. Melninkaitis, and V. Sirutkaitis, Proc. SPIE **6720,** 67200Y (2007).
13. M. Albisi, F. De Tomasi, M. R. Perrone, M. L. Protopapa, A. Rizzo, F. Sarto, and S. Scaglione, Thin Solid films **396,** 44 (2001).
14. X. Jing, J. Shao, J. Zhang, Y. Jin, H. He, and Z. Fan, Opt. Express **17,** 24137 (2009).
15. K. Starke, D. Ristau, H. Welling, T. V. Amotchkina, M. Trubetskov, A. A. Tikhonravov, and A. S. Chirkin, Proc. SPIE **5273,** 501 (2004).
16. L. V. Keldysh, Sov. Phys. JETP **20,** 1307 (1965).
17. M. Jupé, L. Jensen, A. Melninkaitis, V. Sirutkaitis, and D. Ristau, Opt. Express **17,** 12269 (2009).